NASA Technical Memorandum 106700

Solar Radiation on Mars: Tracking Photovoltaic Array

Joseph Appelbaum and Dennis J. Flood
Lewis Research Center
Cleveland, Ohio

and

Marcos Crutchik
Tel Aviv University
Tel Aviv, Israel

September 1994

National Aeronautics and
Space Administration

SOLAR RADIATION ON MARS:
TRACKING PHOTOVOLTAIC ARRAY

J. Appelbaum*, D.J. Flood
National Aeronautics and Space Administration
Lewis Research Center
Cleveland, Ohio 44135

and

M. Crutchik
Faculty of Engineering
Tel Aviv University
Tel Aviv, Israel 69978

ABSTRACT

A photovoltaic power source for surface-based operation on Mars can offer many advantages. Detailed information on solar radiation characteristics on Mars and the insolation on various types of collector surfaces are necessary for effective design of future planned photovoltaic systems. In this article we present analytical expressions for solar radiation calculation and solar radiation data for single axis (of various types) and two axis tracking surfaces and compare the insolation to horizontal and inclined surfaces. For clear skies (low atmospheric dust load) tracking surfaces result in higher insolation than stationary surfaces, whereas for highly dusty atmospheres, the difference is small. The insolation on the different types of stationary and tracking surfaces depend on latitude, season, optical depth of the atmosphere, and the duration of system operation. These insolations have to be compared for each planned mission.

NOMENCLATURE

al Mars surface albedo

G global irradiance

G_{al} irradiance due to albedo

G_b beam irradiance

G_h, G_{bh}, G_{dh}	global, beam and diffuse irradiance on a horizontal surface, respectively
G_β	global irradiance on an inclined surface
H_h, H_{2x}, H_β	daily global insolation on a horizontal, 2 axis and inclined surface, respectively
L_s	areocentric longitude (position of Mars in orbit around the Sun)
z	zenith angle
β	inclination, the angle between the surface and the horizontal
β_p	optimal inclination angle of a surface for a given period
β_y	yearly optimal inclination angle of a surface
γ_c	surface azimuth angle
γ_s	solar azimuth; south zero, east negative, west positive
δ	declination angle, the angular position of the Sun at solar noon with respect to the plane of the equator
δ_p	average declination angle for a given period
θ	Sun angle of incidence
τ	Mars optical depth
ϕ	geographic latitude; north positive, south negative
ω	hour angle; noon zero, morning negative, afternoon positive

INTRODUCTION

The exploration of Mars will require electric power. Of several possibilities direct conversion of solar energy by photovoltaic cells can offer many advantages. To design a photovoltaic system, detailed information on solar radiation data on the Martian surface is necessary.

A photovoltaic array mechanism may either be stationary or tracking. The solar radiation on stationary surfaces on Mars were analyzed in Ref. 1. The present article is a continuation of Ref. 1 and deals with solar radiation calculation on tracking surfaces: single and two axis. The solar radiation model for Mars and the solar radiation calculation procedure have been published in Ref. 2.

2

The type of surface mechanism (stationary or tracking) for the use on Mars is dependent upon the season, latitude and optical depth of Mars atmosphere; the latter is very dominant. Sun tracking surfaces operate better under clear sky conditions (large component of beam irradiance) and the difference in operation is small both for stationary and tracking surfaces for cloudy (dusty) conditions (large component of diffuse irradiance). When the Sun is tracked, the Sun angle of incidence on the surface is reduced (single axis tracking) or zero (two axis tracking) through the day resulting in increased daily isolation relative to stationary (horizontal or inclined) surfaces.

Important engineering trade-off aspects as mass, complexity and reliability of the required drives and controls of the tracking systems will not be addressed in this article. Discussion of photovoltaic array considerations with respect to temperature effects, various types of solar cells, cell efficiencies, dust accumulation and other related issues are reported in Ref. 1. and will not be repeated.

Several possibilities of single axis tracking surface may be implemented: axis may be vertical, horizontal or inclined. The solar insolation of these tracking surfaces depend on the latitude, season, opacity and operating period. Therefore all possible single axis tracking surfaces, as well as the two axis tracking, horizontal and inclined surfaces have to be analyzed and compared for the planned missions. Analytical expression of solar angles and surface parameters are conveniently summarized in this article for tracking surfaces. Some expressions may be found in the literature, some however, are new derivatives. The solar expressions are in general forms and pertain to Mars as well as to Earth. A Mars day, however, is longer than a terrestrial day. Thus, one Mars hour (H) = 1.027 terrestrial hours (hr). The insolation in this article is given in Whr or KWhr (terrestrial hours). The solar radiation model for Mars assumes isotropic skies, therefore, the insolation on the surfaces takes into account this type of distribution for the diffuse light.

The calculation of solar radiation reaching a surface involves trigonometric relationships between the position of the Sun in the sky and the surface parameters. The global irradiance G, in W/m^2, on a surface is the sum of the direct beam irradiance G_b, the diffuse irradiance G_d, and the irradiance due to albedo G_{al}:

$$G = G_b + G_d + G_{al} \qquad (1)$$

For a horizontal surface $G_{al} = 0$ and the irradiance is:

$$G_h = G_{bh} + G_{dh} \qquad (2)$$

For isotropic skies, the global irradiance G_β on an inclined surface with an angle β, is:

$$G_\beta = G_b \cos\theta + G_{dh} \cos^2(\beta/2) + al\, G_h \sin^2(\beta/2) \qquad (3)$$

where θ is the Sun angle of incidence, the angle between the beam irradiance on the surface and the normal to that surface, al is the albedo.

The Sun angle of incidence on a surface in terms of the Sun and surface angles is given by:

$$\cos\theta = \cos\beta\cos z + \sin\beta\sin z\cos(\gamma_s - \gamma_c) \qquad (4)$$

where the solar zenith angle is given by:

$$\cos z = \sin\phi\sin\delta + \cos\phi\cos\delta\cos\omega \qquad (5)$$

As shown by Eq. (3), the irradiance on a surface is a function of the Sun incidence angle θ and the surface inclination angle β. These two angles will be determined for all types of tracking surfaces.

TRACKING SURFACES

Tracking surfaces may by classified by the mode of motion. Motion can be about a single or two axis. The surface tracks the Sun by minimizing the angle of incidence θ, thus tracking algorithms are based on the beam irradiance.

4

TWO AXIS TRACKING

The Sun angle of incidence on a two axis tracking surface is $\theta = 0$, i.e.,

$$\cos\theta = 1 \qquad (6)$$

and the surface inclination angle β equals the zenith angle z, i.e.,

$$\beta = z \qquad (7)$$

SINGLE AXIS TRACKING

Several possibilities of single axis tracking may be implemented. The axis may be vertical, horizontal or inclined.

Vertical Axis

Figure 1 shows a vertical axis-azimuth tracking surface. The surface is inclined at a given angle β. Since the surface tracks the Sun azimuthally we have:

$$\gamma_c = \gamma_s \qquad (8)$$

and from Eq. (4) we have:

$$\cos\theta = \cos(z - \beta) \qquad (9)$$

where the zenith angle is given by Eq. (5). The optimal inclination angle β may be determined for two cases: (1) maximum beam irradiance at solar noon, and (2) maximum daily beam insolation.

For case (1) we get:

$$\beta = \phi - \delta \qquad (10)$$

5

or

$$\beta_p = \phi - \delta_p \qquad (11)$$

where δ_p is the average declination angle for a given period. For a period of one year:

$$\beta_y = \phi \qquad (12)$$

For case (2), the optimal inclination angle is obtained from the beam insolation, Eq. (39)[2].

For the particular case of a vertical surface, $\beta = 90°$ we get:

$$\cos\theta = \sin z \qquad (13)$$

Horizontal Axis

Several tracking modes are possible depending on the orientation of the horizontal axis; whether East-West or North-South.

(a) East-West horizontal axis: North-South tracking. Two possible tracking modes may be applied: (1) Sun altitude tracking, (2) surface tracking for maximum beam irradiance.

For case (1) the Sun altitude tracking, Fig. 2, we obtain for the incidence angle[3]:

$$\cos\theta = (1 - \cos^2\delta\cos^2\omega)^{1/2} \qquad (14)$$

and for the surface inclination angle:

$$\beta = z \qquad (15)$$

For the case (2), the maximum beam irradiance is obtained for minimum incidence angle θ. This angle for an inclined surface facing the equator is given by[3]:

$$\cos\theta = \sin\delta\sin(\phi-\beta) + \cos\delta\cos(\phi-\beta)\cos\omega \qquad (16)$$

Differentiation of Eq. (16) with respect to β, we obtain the optimal inclination angle:

$$\tan\beta = \frac{\sin\phi\cos\delta\cos\omega - \cos\phi\sin\delta}{\sin\phi\sin\delta + \cos\phi\cos\delta\cos\omega} \qquad (17)$$

The solar incidence angle is given by Eq. (16) where β is the angle in Eq. (17).

In both cases of (a) the tracking is nonlinear.

(b) North-South horizontal axis: East-West tracking. This type of tracking is shown in Fig. 3. Two possibilities may be implemented (1) tracking with a constant rotational speed, (2) tracking for maximum beam irradiance.

For constant rotational tracking speed (case (1)) we have[3]:

$$\cos\theta = [(\sin\phi\sin\delta + \cos\phi\cos\delta\cos\omega)^2 + \cos^2\delta\sin^2\omega]^{1/2} \qquad (18)$$

and

$$\beta = \omega \qquad (19)$$

Tracking for maximum beam irradiance (case (2)) is obtained by differentiation of the incidence angle θ with respect to β. The incidence angle is given by:

$$\cos\theta = \sin\beta\cos\delta\sin\omega + \cos\beta(\sin\delta\sin\phi + \cos\delta\cos\phi\cos\omega) \qquad (20)$$

7

The optimal inclination angle is therefore given by:

$$\tan\beta = \frac{\cos\delta\sin\omega}{\sin\phi\sin\delta + \cos\phi\cos\delta\cos\omega} \tag{21}$$

where β is negative in the morning and positive in the afternoon, Fig. 8

Inclined Axis

(a) North-South axis set at inclination angle ψ: East-West tracking. This type of tracking is shown in Fig. 5. The solar incidence angle on the surface, for constant rotational tracking speed, is given by:

$$\cos\theta = \cos\delta\{\sin^2\omega + [\cos(\psi - \phi)\cos\omega - \tan\delta\sin(\psi - \phi)]^2\}^{1/2} \tag{22}$$

and the inclination angle is:

$$\cos\beta = \cos\omega\cos\psi \tag{23}$$

The angle ψ takes different values. A special case is $\psi = \phi$ which is discussed next in (b). Another case is $\psi = \phi - \delta$. The solar incidence angle in this case becomes:

$$\cos\theta = \cos\delta\{\sin^2\omega + [\cos\delta\cos\omega + \tan\delta\sin\delta]^2\}^{1/2} \tag{24}$$

and the inclination angle is:

$$\cos\beta = \cos\omega\cos(\phi - \delta) \tag{25}$$

(b) North-South axis set at latitude inclination angle: East-West polar tracking. This is a particular case[3] where $\psi = \phi$ i.e., the surface is inclined from the horizontal at local latitude. The solar incidence on the surface is obtained from Eq. (22) for $\psi = \phi$, i.e.,

8

$$\cos\theta = \cos\delta \qquad (26)$$

and the inclination angle is:

$$\cos\beta = \cos\omega\cos\phi \qquad (27)$$

SOLAR RADIATION ON TRACKING SURFACES

The global irradiance on an inclined surface is given by Eq. (3). For tracking surfaces, the angle θ and β vary during the day according to an algorithm depending on the tracking mode. The tracking modes are based on the direct beam irradiance, however, the surface also collects diffuse and reflected irradiances. By integrating the irradiances over the day (Eqs. (15–22))[2] we obtain the daily insolation. In this section we calculate and compare the insolation on tracking surfaces for the different tracking modes.

Two Axis Tracking

For 2 axis tracking, $\cos\theta = 1$ and $\beta = z$ (Eqs. (6) and (7)) and the global irradiance (Eq. (3)) is given by:

$$G_{2x} = G_b + G_{dh}\cos^2(z/2) + al\,G_h\sin^2(z/2) \qquad (28)$$

The variation of the daily global insolation H_{2x} on a 2 axis tracking surface at VL1 ($\phi = 22.3°N$) and VL2 ($\phi = 47.7°N$) for the observed opacities on Mars by the Viking lander cameras[2] is shown in Fig. 6. The season is indicated by the value of L_s areocentric longitude of the Sun, measured in the orbital plane of the planet from its vernal equinox, $L_s = 0$. A comparison of the daily global insolation on a horizontal surface H_h, on an inclined surface H_β at $\beta = \phi$ and on a 2 axis tracking surface H_{2x} for the observed opacities at VL1 and VL2 is shown in Fig. 7. There is a noticeable difference in the isolation for the three cases during the spring and summer where the optical depth is relatively low, and there is only a small difference in insolation during the autumn and winter where the optical depth is high. For a yearly operation, the average gain in insolation is about 7 percent at VL1 and 21 percent at VL2 for the 2 axis tracking surface compared to the horizontal surface. There is a small difference in the average yearly operation between a horizontal and an inclined surface at the local latitudes of VL1 and VL2.

In Fig. 8 we show the variation of the daily global insolation H_{2x} on a 2 axis tracking surface at VL1 and VL2 for clear skies with $\tau = 0.5$. The effect of the global storms ($L_s = 180°$ to $360°$) can be noticed by comparing Figs. 6 and 8. The daily insolation components (in Whr/m^2): B- beam, D- diffuse and A- albedo, as well as the daily global insolation G for 2 axis tracking surface at VL1 are shown in Table 1 for the observed opacities and for $\tau = 0.5$. The variation of the daily global insolation in Whr/m^2 for the entire planet for 2 axis tracking surface may be of interest. For this purpose we resort to the optical depth model $\tau (\phi, L_s)^2$. The results are shown in Fig. 9. It is also interesting to compare the insolation for the entire planet for clear skies with $\tau = 0.5$ through the year, Fig. 10.

Single Axis Tracking

The operation of the various single axis tracking surfaces will now be compared. Two possible tracking modes may be applied for each of the East-West and North-South horizontal axis. The daily global insolation for a Martian year for the observed opacities was calculated for six single axis tracking modes: (1) Azi-Opt (vertical axis, azimuth tracking), (2) NST_{r1} (East-West horizontal axis: North-South tracking; Sun altitude tracking), (3) NST_{r2} (East-West horizontal axis: North-South tracking; maximum beam irradiance), (4) EWT_{r1} (North-South horizontal axis: East-West tracking; constant rotational tracking speed), (5) EWT_{r2} (North-South horizontal axis: East-West tracking; maximum beam irradiance), and (6) EWPol (North-South axis: East-West polar tracking). The results show that NST_{r2} produces higher insolation and there is almost no difference between EWT_{r1} and EWT_{r2}. Therefore, four modes of single tracking surfaces will further be investigated: (1) Azi-Opt (Eqs. (9) and (12)), (2) NST_{r2} (Eqs. (16) and (17)), (3) EWT_{r1} (Eqs. (18) and (19)) and (4) EWPol (Eqs. (26) and (27)) . The performance of these single axis tracking surfaces will be compared to a 2 axis tracking, a horizontal surface (horiz) and an inclined surface with $\beta = \phi - \delta$ (Beta). Table 2 shows this comparison for VL1 for the observed opacities and Table 3 for clear skies with $\tau = 0.5$. Based on the average yearly insolation for the observed opacities, the best tracking modes are the two axis, EWT_{r1} and EWPol as compared to the horizontal surface. The difference in isolation for these three modes is small indicating of no significant advantage of the 2 axis tracking. For clear skies, however, the difference in average yearly insolation is larger: the gain for the 2 axis tracking is 19.1 percent, 15.9 percent for EWPol, 13.1 percent for Azi-Opt, 13.0 percent for $EWTr_1$, and 8.3 percent for NST_{r2} as compared to a horizontal surface. The variation of

daily insolation of the different tracking modes for clear skies with $\tau = 0.5$ at VL1 is shown in Fig. 11.

The diurnal variation of the irradiance for the tracking modes for $L_s = 141°$ (lowest observed opacity) at

VL1 is shown in Fig. 12. Finally, the operation of a single tracking surface for the entire planet is shown

in Figs. 13(a) and (b) for the EWPol tracking (inclination angle at local latitudes) for the optical depth

model $\tau (\phi, L_s)^2$ and for clear skies with $\tau = 0.5$, respectively.

CONCLUSIONS

Utilization of solar energy on Mars depends on adequate knowledge of solar radiation

characteristics in the region of system operation. This article deals with solar radiation calculation on one

and two axis tracking surfaces and is based on the solar radiation model developed in Ref. 2. The

operation of these tracking surfaces was also compared to the operation of stationary surfaces (horizontal

and inclined).

Sun tracking surfaces operate better under clear skies, Figs. 7 and 11 and the difference in

insolation is small for dusty atmospheres, Fig. 7. Based on the average yearly insolation at VL1 for the

observed opacities the two axis tracking surface and the single axis EWT_{r1} (North-South horizontal axis:

East-West tracking) and EWPol (North-South axis: East-West polar tracking) resulted in the highest

insolation. For clear skies ($\tau = 0.5$) the gain in average yearly insolation is 19.1 percent for the 2 axis

tracking, 15.9 percent for EWPol and 13.0 percent for EWT_{r1} as compared to a horizontal surface at VL1.

However, it should be noted that the insolation on the different types of stationary and tracking surfaces

depend on the latitude, season, optical depth of the atmosphere and the duration of system operation.

These insolations have to be compared for each planned mission.

REFERENCES

[1]Appelbaum, J., Sherman, I., and Landis, G.A., "Solar Radiation on Mars: Stationary Photovoltaic

Array," accepted for publication in AIAA.

[2]Appelbaum, J., Landis, G.A., and Sherman, I., "Solar Radiation on Mars—Update 1991," Solar Energy,

Vol. 50, No. 1, 1993, pp. 35–51.

[3]Duffie, J.A., and Beckman, W.A., "Solar Engineering of Thermal Processes," John Wiley & Sons, New

York, Chichester, Brisbane, Toronto, Singapore, p. 15.

Table 1.—Daily insolation in Whr/m^2 (global G, beam B, diffuse D and albedo A) on a 2 axis tracking surface at VL1 for the observed opacities and for $\tau = 0.5$.

	observed opacities					$\tau = 0.5$			
Ls	G_2_axis	B_2_axis	D_2_axis	A_2_axis	Ls	G_2_axis	B_2_axis	D_2_axis	A_2_axis
0	3647.7	2130.0	1428.2	89.5	0	4010.8	2665.7	1250.0	95.1
5	3220.3	1507.4	1634.0	78.8	5	4027.4	2676.3	1259.0	92.1
10	3495.7	1870.6	1544.2	80.8	10	4040.0	2684.4	1266.3	89.3
15	3810.9	2324.6	1403.0	83.3	15	4050.0	2690.6	1272.5	86.9
20	3718.1	2171.3	1467.1	79.7	20	4058.4	2695.1	1278.5	84.8
25	3727.3	2176.9	1472.6	77.8	25	4063.5	2698.5	1282.3	82.7
30	3948.5	2512.5	1356.6	79.5	30	4068.1	2701.0	1285.9	81.2
35	3842.6	2343.0	1423.1	76.5	35	4071.8	2703.2	1288.7	79.9
40	4075.5	2705.3	1291.2	79.0	40	4075.5	2705.3	1291.2	79.0
45	3752.4	2190.7	1488.0	73.7	45	4080.3	2707.8	1294.0	78.5
50	3663.0	2048.5	1542.7	71.8	50	4084.9	2711.2	1295.7	78.0
55	3346.8	1571.8	1708.7	66.3	55	4091.9	2715.7	1298.4	77.8
60	3678.1	2056.7	1549.7	71.7	60	4100.9	2721.5	1301.5	77.9
65	3783.4	2208.6	1501.4	73.4	65	4112.5	2729.0	1305.3	78.2
70	3897.7	2375.4	1447.1	75.2	70	4126.7	2738.3	1309.8	78.6
75	4024.8	2559.5	1388.0	77.3	75	4144.0	2749.7	1315.2	79.0
80	4044.3	2571.9	1394.6	77.9	80	4164.2	2763.1	1321.5	79.5
85	4067.1	2586.3	1402.4	78.4	85	4187.8	2778.7	1329.0	80.1
90	3876.1	2262.4	1538.0	75.7	90	4214.5	2796.4	1337.4	80.6
95	3805.0	2127.2	1603.1	74.7	95	4244.0	2816.1	1346.8	81.2
100	3834.1	2143.5	1615.4	75.2	100	4276.3	2837.5	1357.1	81.7
105	4311.0	2860.6	1368.2	82.2	105	4311.0	2860.6	1368.2	82.2
110	4347.4	2884.8	1379.9	82.8	110	4347.4	2884.8	1379.9	82.8
115	4671.7	3372.2	1212.4	87.2	115	4385.1	2909.8	1391.9	83.4
120	4712.1	3401.6	1222.7	87.9	120	4423.2	2935.3	1403.8	84.1
125	4752.6	3431.0	1232.9	88.7	125	4461.1	2960.7	1415.5	84.9
130	4792.4	3459.9	1242.7	89.8	130	4498.0	2985.4	1426.7	85.9
135	4831.6	3487.7	1252.7	91.1	135	4533.9	3008.9	1437.8	87.2
140	5041.4	3793.1	1153.6	94.7	140	4565.4	3030.5	1446.4	88.5
145	4593.8	3049.8	1453.9	90.1	145	4593.8	3049.8	1453.9	90.1
150	4239.5	2475.9	1677.0	86.6	150	4617.6	3065.9	1459.6	92.1
155	4251.9	2483.2	1679.9	88.7	155	4635.4	3078.2	1462.8	94.4
160	4145.5	2318.3	1737.7	89.5	160	4647.5	3086.4	1464.0	97.1
165	4140.6	2315.8	1732.7	92.0	165	4650.7	3089.7	1461.3	99.7
170	4020.8	2151.6	1776.2	93.0	170	4646.9	3087.7	1456.5	102.8
175	3997.9	2138.3	1763.6	95.9	175	4634.9	3080.0	1448.9	106.0
180	3964.9	2119.9	1746.0	99.0	180	4613.4	3066.3	1437.8	109.4
185	3369.2	1372.2	1905.5	91.4	185	4582.5	3046.2	1423.5	112.8
190	3092.2	1092.1	1910.7	89.3	190	4542.3	3019.8	1406.4	116.1
195	3167.4	1223.6	1848.9	95.0	195	4493.1	2987.3	1386.6	119.3
200	3250.2	1375.0	1774.6	100.7	200	4434.4	2948.6	1363.5	122.3
205	2262.8	372.5	1767.7	122.5	205	4368.8	2904.4	1339.2	125.2
210	1840.3	153.8	1562.2	124.4	210	4294.7	2855.3	1311.9	127.5
215	1933.8	216.7	1582.1	134.9	215	4214.8	2802.1	1283.3	129.4
220	1905.0	232.9	1539.0	133.0	220	4130.3	2745.6	1253.8	130.9
225	1876.4	251.6	1494.6	130.3	225	4043.1	2687.1	1223.9	132.1
230	1908.6	318.3	1466.8	123.5	230	3954.5	2628.0	1193.6	132.8
235	1891.2	349.8	1422.1	119.3	235	3866.3	2569.7	1163.7	133.0
240	1888.4	387.8	1385.5	115.1	240	3782.1	2513.5	1135.8	132.8
245	1937.3	471.4	1357.3	108.6	245	3704.0	2461.0	1110.5	132.5
250	2007.8	581.7	1325.0	101.1	250	3633.9	2413.5	1088.4	132.0
255	2130.8	728.7	1302.1	100.0	255	3573.1	2372.5	1069.3	131.3
260	2088.8	711.6	1277.9	99.3	260	3522.7	2338.6	1053.5	130.6
265	1764.3	416.4	1242.4	105.5	265	3484.4	2312.9	1041.6	129.8
270	1526.9	227.9	1181.8	117.3	270	3458.6	2295.7	1033.8	129.1
275	1224.0	71.9	1033.1	119.0	275	3445.5	2287.1	1030.0	128.4
280	1085.0	38.4	940.7	105.8	280	3444.7	2286.8	1030.2	127.7
285	1204.1	64.3	1024.9	114.8	285	3455.7	2294.5	1034.1	127.0
290	921.6	14.1	819.7	87.8	290	3476.6	2309.1	1041.2	126.3
295	1054.3	28.2	928.7	97.4	295	3506.3	2329.7	1051.2	125.4
300	1144.6	41.3	1001.1	102.2	300	3543.8	2355.1	1064.2	124.5
305	1331.5	81.7	1136.1	113.7	305	3587.2	2384.1	1079.7	123.4
310	1607.3	185.7	1299.0	122.7	310	3634.6	2415.4	1097.1	122.1
315	1937.7	417.1	1415.0	105.6	315	3683.1	2447.9	1114.9	120.3
320	2154.9	589.9	1468.3	96.7	320	3731.5	2480.5	1132.7	118.3
325	2261.1	661.4	1506.6	93.1	325	3778.7	2512.2	1150.5	116.0
330	2419.8	794.5	1538.1	87.1	330	3823.7	2542.1	1168.0	113.5
335	2600.0	948.4	1565.2	86.4	335	3865.6	2569.9	1184.9	110.8
340	2539.1	845.4	1610.7	83.0	340	3902.7	2595.0	1200.0	107.6
345	3153.3	1535.8	1526.4	91.1	345	3936.6	2617.2	1214.8	104.5
350	2959.7	1259.4	1616.8	83.5	350	3965.5	2636.4	1227.8	101.3
355	3322.7	1698.0	1537.5	87.2	355	3990.2	2652.5	1239.5	98.2
360	3647.7	2130.0	1428.2	89.5	360	4010.8	2665.7	1250.0	95.1

Table 2.—Daily insolation in Whr/m² on a 2 axis tracking surface, horizontal surface (horiz), inclined surface with $\beta = \phi - \delta$ (Beta), and four modes of single axis tracking surfaces at VL1 for the observed opacities.

Ls	2_axis	Horiz	Beta	Azi_Opt	N_S_Tr2	E_W_Tr1	E_W_Pol
0.0	3647.7	3262.1	3355.6	3602.5	3418.5	3564.5	3647.7
5.0	3220.3	3057.1	3093.5	3247.7	3157.1	3182.5	3211.1
10.0	3495.7	3230.0	3270.8	3463.9	3342.5	3451.8	3476.8
15.0	3810.9	3405.5	3446.0	3685.4	3524.1	3764.4	3780.8
20.0	3718.1	3378.2	3400.3	3603.7	3477.6	3684.4	3673.0
25.0	3727.3	3395.2	3406.4	3591.8	3483.4	3700.1	3665.8
30.0	3948.5	3512.4	3516.7	3713.9	3598.0	3923.5	3866.5
35.0	3842.6	3471.2	3468.5	3624.3	3545.8	3821.3	3742.0
40.0	4075.5	3586.0	3578.4	3733.3	3662.9	4053.9	3946.8
45.0	3752.4	3440.0	3433.0	3526.7	3502.5	3730.3	3613.8
50.0	3663.0	3396.6	3390.4	3453.3	3454.3	3638.5	3509.4
55.0	3346.8	3216.0	3212.7	3241.5	3261.3	3319.9	3195.7
60.0	3678.1	3412.3	3410.0	3427.4	3469.1	3646.2	3489.0
65.0	3783.4	3472.0	3472.5	3468.9	3534.7	3746.6	3570.3
70.0	3897.7	3534.0	3538.0	3512.2	3604.9	3855.5	3660.3
75.0	4024.8	3601.5	3609.2	3561.2	3683.0	3977.1	3762.8
80.0	4044.3	3618.4	3629.0	3565.7	3702.4	3993.1	3771.4
85.0	4067.1	3638.4	3650.9	3577.9	3724.3	4013.6	3786.7
90.0	3876.1	3555.7	3566.5	3501.6	3625.2	3825.4	3616.3
95.0	3805.0	3528.9	3538.3	3480.6	3591.7	3756.0	3556.0
100.0	3834.1	3556.2	3564.3	3513.6	3618.8	3786.5	3588.2
105.0	4311.0	3802.1	3811.1	3756.6	3897.1	4259.4	4025.7
110.0	4347.4	3834.8	3840.0	3807.7	3927.1	4299.9	4074.1
115.0	4671.7	3984.6	3985.4	3979.4	4096.5	4625.8	4389.1
120.0	4712.1	4019.1	4014.6	4046.4	4125.8	4672.3	4451.1
125.0	4752.6	4052.9	4043.7	4117.2	4154.8	4718.7	4516.1
130.0	4792.4	4084.7	4072.4	4190.2	4183.1	4763.3	4582.5
135.0	4831.6	4115.0	4102.1	4265.5	4211.3	4805.6	4649.5
140.0	5041.4	4202.7	4190.3	4421.4	4308.2	5015.9	4882.5
145.0	4593.8	4035.1	4031.6	4242.0	4127.3	4568.5	4474.9
150.0	4239.5	3870.3	3873.8	4061.0	3959.8	4213.4	4149.3
155.0	4251.9	3873.0	3885.9	4097.3	3973.7	4220.9	4181.7
160.0	4145.5	3811.0	3833.2	4046.4	3919.8	4109.8	4093.8
165.0	4140.6	3795.0	3831.4	4061.0	3917.6	4095.9	4105.2
170.0	4020.8	3715.2	3762.2	3984.2	3844.6	3970.3	3999.1
175.0	3997.9	3681.7	3746.1	3976.8	3823.5	3935.4	3988.2
180.0	3964.9	3637.9	3721.8	3958.0	3791.1	3888.6	3965.0
185.0	3369.2	3267.4	3307.6	3448.0	3358.9	3331.3	3379.1
190.0	3092.2	3062.7	3084.7	3192.2	3122.7	3071.6	3112.4
195.0	3167.4	3088.5	3134.4	3258.9	3164.2	3128.1	3194.4
200.0	3250.2	3107.8	3187.3	3331.2	3209.4	3183.9	3280.3
205.0	2262.8	2371.7	2327.3	2356.8	2353.5	2303.2	2308.0
210.0	1840.3	1974.1	1906.5	1916.8	1929.3	1902.0	1889.0
215.0	1933.8	2059.4	1995.2	2010.3	2013.1	1992.9	1989.7
220.0	1905.0	2032.7	1964.8	1980.9	1975.0	1968.0	1968.8
225.0	1876.4	2004.5	1934.1	1951.5	1937.5	1942.0	1947.4
230.0	1908.6	2028.2	1963.3	1985.7	1958.6	1969.9	1986.6
235.0	1891.2	2003.5	1942.5	1967.0	1932.8	1949.4	1973.6
240.0	1888.4	1991.0	1936.2	1963.4	1922.2	1941.3	1974.0
245.0	1937.3	2015.5	1979.1	2012.7	1960.2	1974.5	2023.4
250.0	2007.8	2047.2	2040.3	2082.9	2017.4	2019.5	2089.9
255.0	2130.8	2109.4	2149.0	2204.2	2124.0	2102.2	2201.5
260.0	2088.8	2069.7	2107.6	2160.7	2082.1	2061.6	2160.0
265.0	1764.3	1849.0	1804.4	1832.0	1783.0	1808.8	1855.1
270.0	1526.9	1656.4	1572.4	1585.9	1557.7	1605.9	1620.2
275.0	1224.0	1367.2	1266.3	1269.9	1259.2	1317.8	1307.6
280.0	1085.0	1225.2	1125.1	1126.9	1118.9	1178.0	1163.0
285.0	1204.1	1345.4	1246.7	1249.9	1240.8	1295.8	1284.1
290.0	921.6	1046.9	958.0	958.6	953.8	1004.2	987.1
295.0	1054.3	1187.6	1095.2	1096.5	1091.7	1140.1	1123.4
300.0	1144.6	1279.7	1188.6	1190.6	1186.4	1229.2	1213.3
305.0	1331.5	1466.6	1379.7	1384.2	1379.6	1412.2	1400.6
310.0	1607.3	1730.0	1658.2	1670.3	1659.4	1674.1	1675.5
315.0	1937.7	2022.1	1983.9	2016.0	1979.3	1975.0	2004.5
320.0	2154.9	2198.1	2189.5	2239.2	2184.9	2166.2	2214.2
325.0	2261.1	2288.0	2289.8	2348.0	2289.2	2262.9	2314.0
330.0	2419.8	2414.6	2434.3	2508.3	2437.3	2405.7	2465.2
335.0	2600.0	2553.7	2592.7	2685.7	2602.3	2568.7	2636.9
340.0	2539.1	2530.7	2548.3	2629.6	2565.1	2525.0	2572.1
345.0	3153.3	2928.2	3027.7	3198.4	3058.3	3069.4	3170.7
350.0	2959.7	2840.9	2892.8	3025.1	2929.2	2914.1	2975.2
355.0	3322.7	3072.3	3152.3	3341.9	3202.1	3252.2	3329.7
360.0	3647.7	3262.1	3355.6	3602.5	3418.5	3564.5	3647.7
AVG	3097.2	2904.3	2899.3	2978.7	2942.5	3089.1	3050.6

13

Table 3.—Daily insolation in Whr/m^2 on a 2 axis tracking surface, horizontal surface (horiz), inclined surface with $\beta = \phi - \delta$ (Beta), and four modes of single axis tracking surfaces at VL1 for clear skies with $\tau = 0.5$.

| Ls	2_axis	Horiz	Beta	Azi_Opt	N_S_Tr2	E_W_Tr1	E_W_Pol
0.0	4010.8	3420.8	3552.0	3881.9	3619.2	3897.4	4010.9
5.0	4027.4	3456.1	3556.7	3876.7	3630.9	3936.5	4020.8
10.0	4040.0	3486.2	3559.6	3866.0	3638.7	3968.6	4023.6
15.0	4050.0	3511.9	3562.3	· 3851.2	3644.0	3994.7	4020.7
20.0	4058.4	3534.5	3565.7	3833.6	3649.0	4016.0	4013.4
25.0	4063.5	3550.9	3567.1	3810.5	3651.4	4030.8	4000.4
30.0	4068.1	3565.2	3570.0	3786.1	3654.7	4041.9	3984.6
35.0	4071.8	3576.5	3573.4	3759.9	3658.3	4049.3	3966.3
40.0	4075.5	3586.0	3578.4	3733.3	3662.9	4053.9	3946.8
45.0	4080.3	3595.0	3585.7	3707.7	3669.6	4057.6	3927.8
50.0	4084.9	3601.4	3592.3	3681.2	3676.5	4059.4	3908.7
55.0	4091.9	3609.2	3602.4	3658.4	3686.2	4062.3	3892.5
60.0	4100.9	3617.8	3614.4	3638.9	3697.8	4066.3	3879.5
65.0	4112.5	3628.0	3628.7	3624.0	3711.7	4072.6	3870.9
70.0	4126.7	3640.2	3645.1	3614.4	3727.8	4081.7	3867.3
75.0	4144.0	3654.8	3663.4	3611.0	3746.1	4094.4	3869.7
80.0	4164.2	3672.0	3683.8	3614.7	3766.4	4110.8	3878.2
85.0	4187.8	3692.4	3706.2	3626.6	3789.0	4132.0	3893.8
90.0	4214.5	3715.8	3730.3	3646.8	3813.7	4157.6	3916.5
95.0	4244.0	3742.0	3756.0	3675.3	3839.9	4187.5	3946.1
100.0	4276.3	3770.8	3782.9	3712.0	3867.7	4221.5	3982.6
105.0	4311.0	3802.1	3811.1	3756.6	3897.1	4259.4	4025.7
110.0	4347.4	3834.8	3840.0	3807.7	3927.1	4299.9	4074.1
115.0	4385.1	3868.5	3869.2	3864.2	3957.7	4342.5	4127.4
120.0	4423.2	3902.1	3898.4	3924.8	3988.4	·4385.8	4184.4
125.0	4461.1	3934.9	3927.4	3988.5	4018.8	·4428.8	4243.7
130.0	4498.0	3965.6	3955.7	4053.6	4048.4	4469.9	4304.0
135.0	4533.9	3994.7	3984.3	4119.9	4077.5	4508.7	4364.4
140.0	4565.4	4017.2	4008.6	4182.1	4103.3	4541.3	4421.3
145.0	4593.8	4035.1	4031.6	4242.0	4127.3	4568.5	4474.9
150.0	4617.6	4046.8	4052.2	4297.5	4148.3	4587.9	4522.8
155.0	4635.4	4050.7	4069.1	4346.8	4165.2	4598.1	4563.4
160.0	4647.5	4047.5	4083.3	4390.1	4178.7	4599.0	4596.0
165.0	4650.7	4032.8	4090.7	4422.4	4184.5	4587.3	4617.1
170.0	4646.9	4009.8	4094.4	4446.8	4185.3	4564.8	4628.1
175.0	4634.9	3977.5	4093.2	4461.6	4178.7	4530.3	4627.3
180.0	4613.4	3934.8	4085.7	4465.2	4163.0	4482.9	4613.5
185.0	4582.5	3881.8	4071.1	4457.3	4138.0	4423.0	4586.3
190.0	4542.3	3819.2	4049.6	4438.1	4106.4	4351.4	4546.4
195.0	4493.1	3748.4	4021.5	4408.1	4068.9	4269.2	4494.2
200.0	4434.4	3668.9	3985.4	4366.4	4024.3	4176.3	4429.4
205.0	4368.8	3584.4	3943.8	4316.3	3974.9	4076.3	4355.2
210.0	4294.7	3492.7	3893.9	4255.2	3918.2	3968.4	4270.6
215.0	4214.8	3397.5	3838.2	4186.5	3856.7	3856.1	4178.7 ·
220.0	4130.3	3300.6	3777.8	4111.9	3790.8	3741.4	4081.5
225.0	4043.1	3203.8	3713.5	4032.7	3722.0	3626.5	3981.3
230.0	3954.5	3108.5	3646.8	3951.1	3651.2	3513.4	3880.0
235.0	3866.3	3015.8	3578.2	3868.1	3579.6	3404.2	3780.0
240.0	3782.1	2929.5	3511.6	3788.1	3510.4	3302.4	3685.0
245.0	3704.0	2851.7	3449.0	3713.3	3445.6	3210.6	3597.8
250.0	3633.9	2783.7	3392.0	3645.7	3386.9	3130.3	3520.3
255.0	3573.1	2726.1	3341.6	3586.7	3335.4	3062.6	3453.9
260.0	3522.7	2679.6	3299.1	3537.5	3292.0	3008.2	3399.6
265.0	3484.4	2645.6	3265.9	3499.8	3258.3	2968.8	3359.2
270.0	3458.6	2624.5	3242.6	3474.1	3235.0	2944.7	3333.3
275.0	3445.5	2616.1	3229.4	3460.7	3222.0	2935.7	3321.7
280.0	3444.7	2620.3	3226.1	3459.2	3219.1	2941.6	3324.3
285.0	3455.7	2636.5	3231.8	3468.9	3225.8	2961.9	3340.3
290.0	3476.6	2663.2	3245.1	3487.9	3240.3	2994.8	3367.9
295.0	3506.3	2699.5	3265.0	3515.2	3261.8	3039.3	3405.8
300.0	3543.8	2744.9	3290.4	3549.4	3289.2	3094.4	3452.8
305.0	3587.2	2798.0	3319.8	3588.8	3321.1	3158.3	3507.0
310.0	3634.6	2857.0	3351.8	3631.5	3355.8	3229.2	3566.2
315.0	3683.1	2918.5	3382.9	3673.7	3390.6	3303.6	3626.8
320.0	3731.5	2981.9	3413.0	3714.8	3424.7	3380.1	3687.3
325.0	3778.7	3046.0	3441.0	3753.3	3457.6	3457.1	3746.4
330.0	3823.7	3109.6	3466.8	3788.5	3488.5	3533.2	3802.2
335.0	3865.6	3171.5	3489.6	3819.2	3517.0	3606.8	3853.6
340.0	3902.7	3228.9	3507.4	3842.8	3541.7	3675.5	3898.3
345.0	3936.6	3284.1	3523.4	3862.0	3564.9	3740.4	3937.5
350.0	3965.5	3334.2	3535.4	3874.5	3585.0	3798.9	3969.1
355.0	3990.2	3380.1	3544.9	3881.2	3603.1	3851.3	3993.6
360.0	4010.8	3420.8	3552.0	3881.9	3619.2	3897.4	4010.9
AVG	4079.4	3425.5	3659.1	3874.9	3710.5	3872.0	3971.4

14
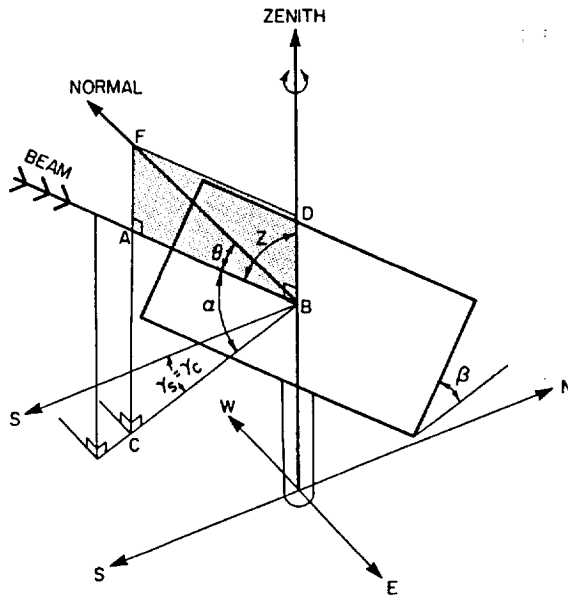
Fig. 1—Vertical axis tracking.
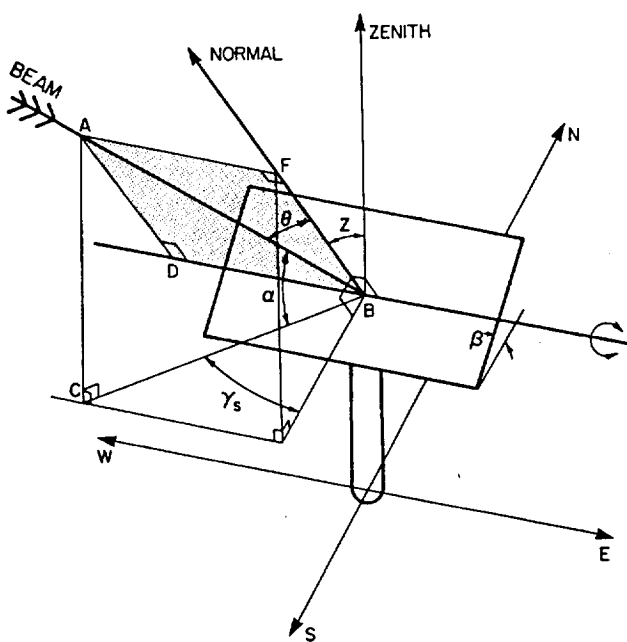
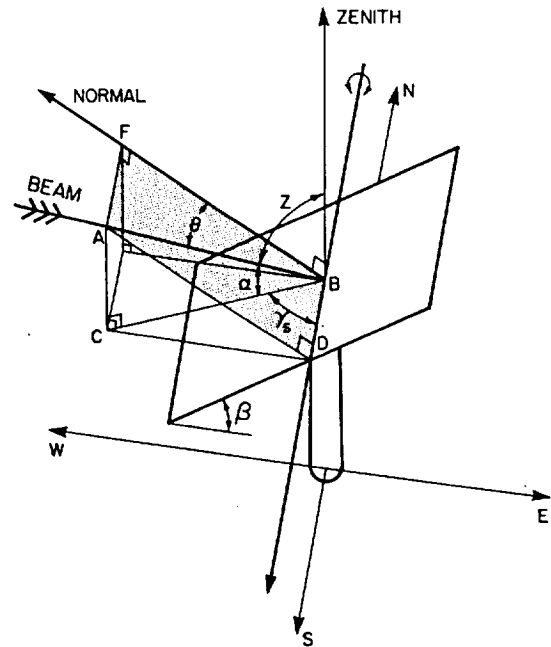Fig. 2.—East-West horizontal axis: North-South tracking.
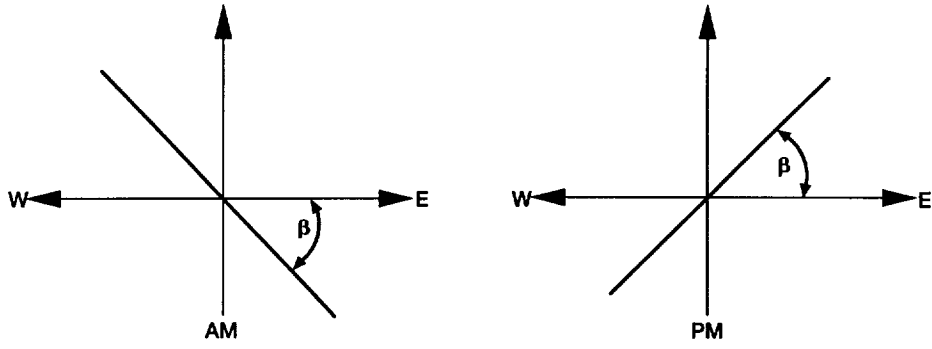
Fig. 3.—North-South horizontal axis: East-West tracking.

15

Fig. 4.—Inclination angle β at morning (AM) and afternoon (PM).
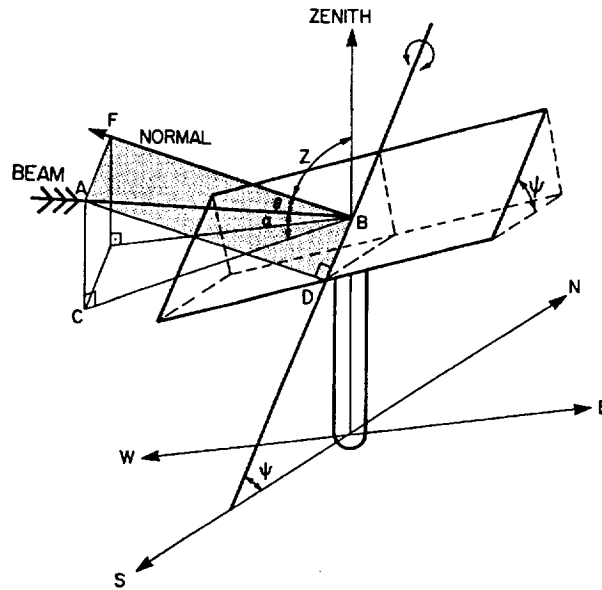

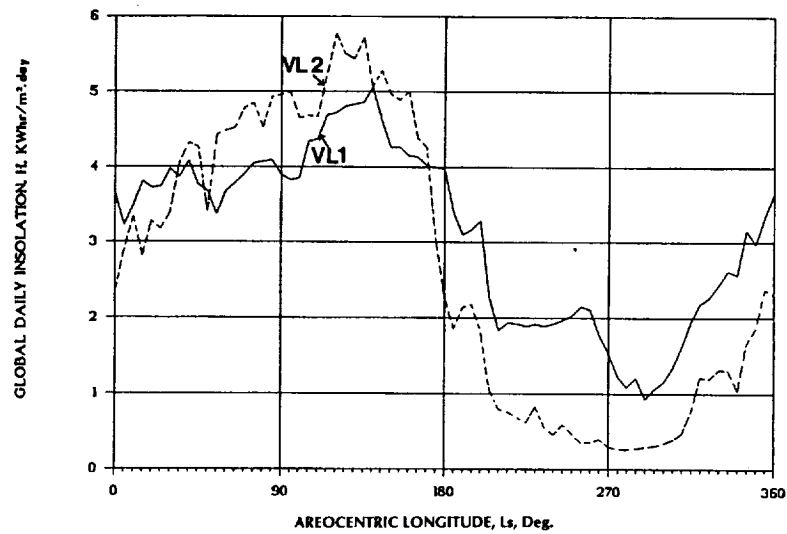Fig. 5.—North-South inclined axis: East-West tracking.

Fig. 6.—Variation of daily global insolation H_{2x} on a 2 axis tracking surface at VL1 and VL2 for observed opacities.
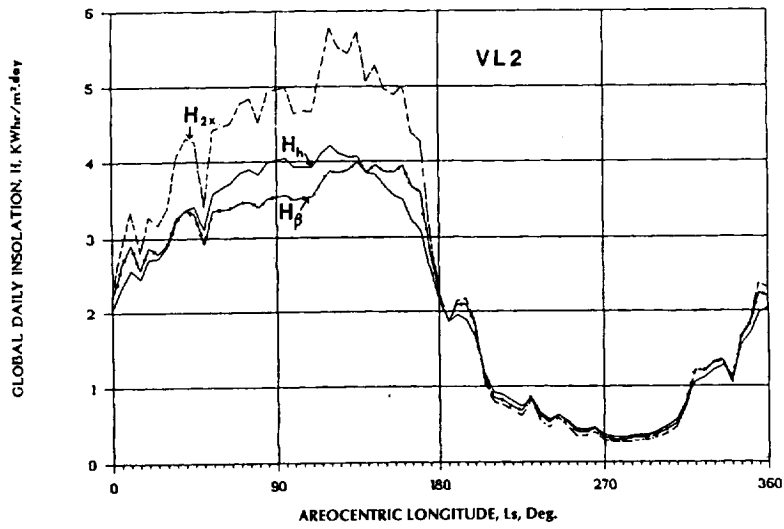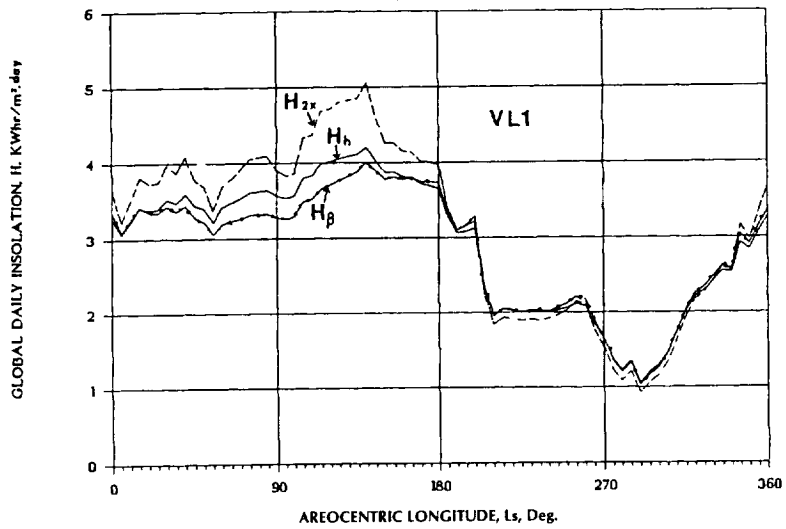
16

Fig. 7.—Variation of daily global insolation on a horizontal surface H_h, inclined surface H_β ($\beta = \phi$); and on 2 axis tracking surface H_{2x} for observed opacities at VL1 and VL2.

17
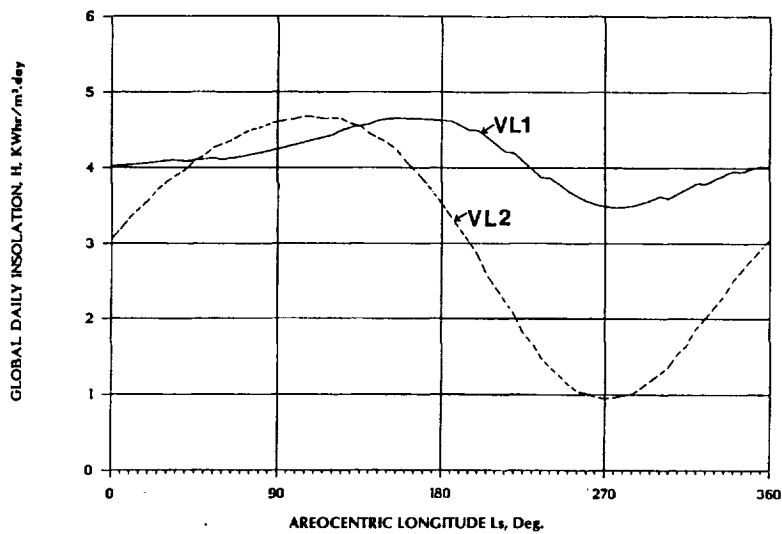
Fig. 8.—Variation of daily global insolation H_{2x} on 2 axis tracking surface at VL1 and VL2 for $\tau = 0.5$.
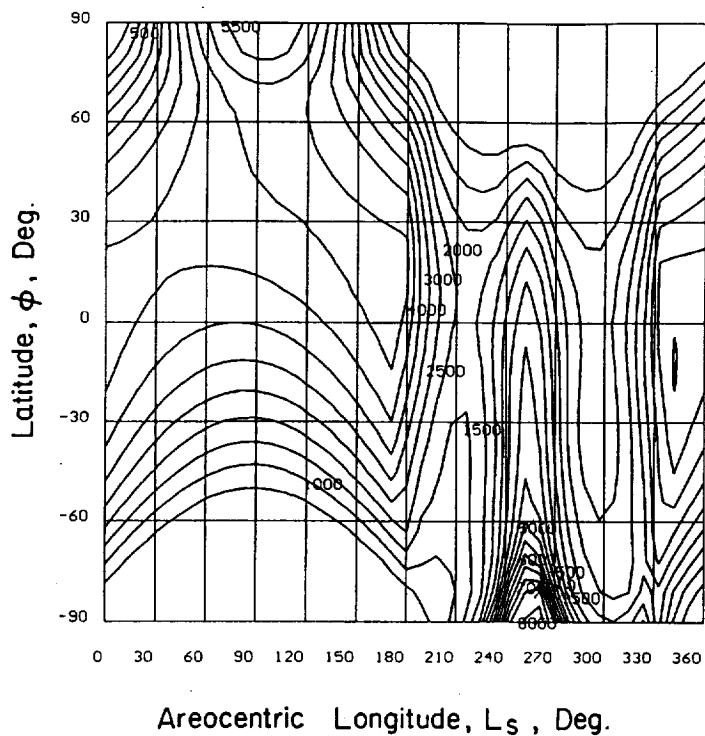
Fig. 9.—Variation of daily global insolation H_{2x} (Whr/m²) with latitude and areocentric longitude on a 2x tracking surface based on optical depth function (Eq. (1))².

18
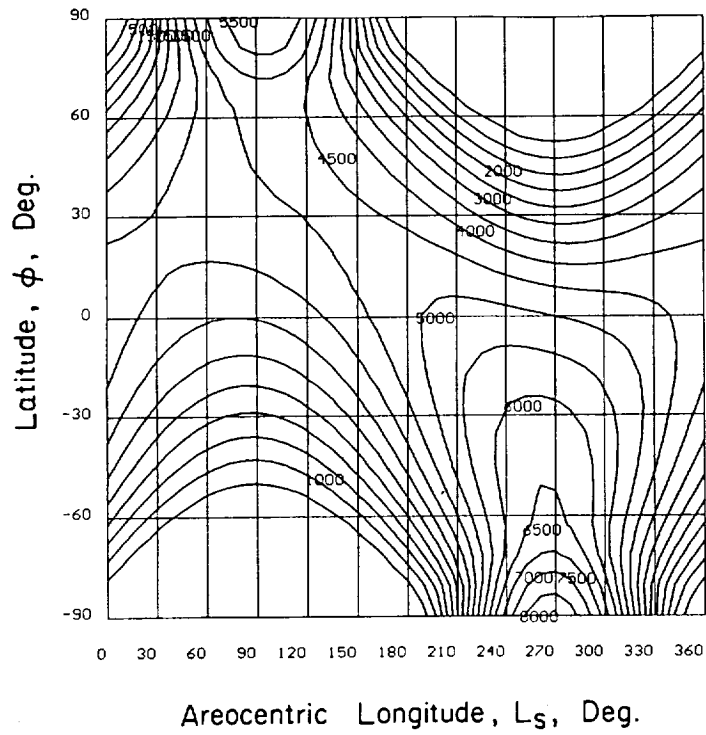
Fig. 10.—Variation of daily global insolation H_{2x} (Whr/m^2) with latitude and areocentric longitude on a 2x tracking surface for clear skies with $\tau = 0.5$.
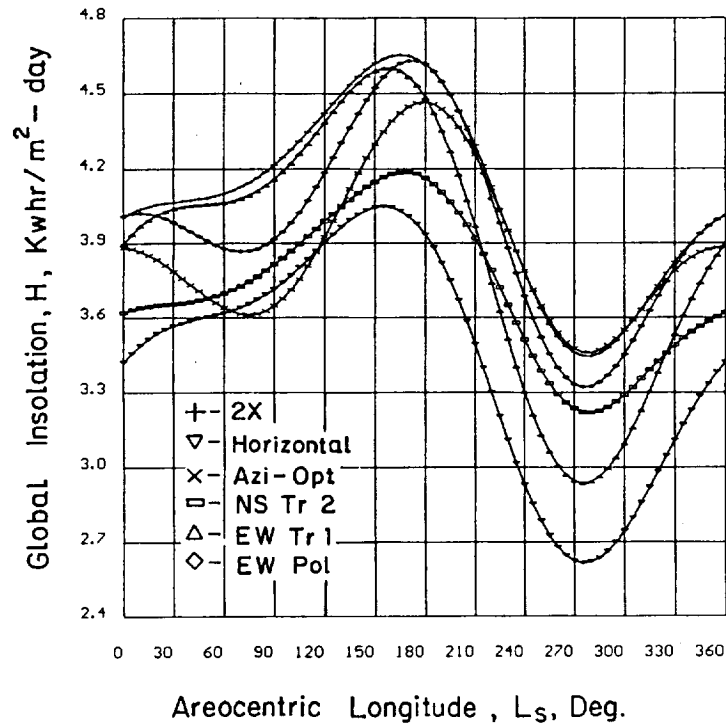
Fig. 11.—Variation of daily global insolation on 2 axis tracking surface, horizontal surface and four modes of single tracking surfaces at VL1 and $\tau = 0.5$.

19
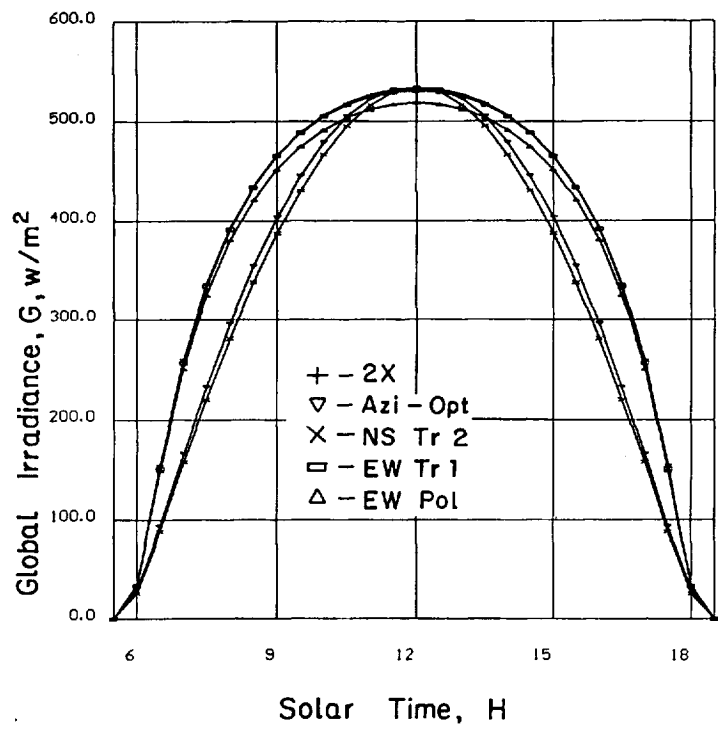
Fig. 12.—Diurnal variation of global irradiance for single axis tracking modes for $L_s = 141°$ (lowest observed opacity) at VL1.
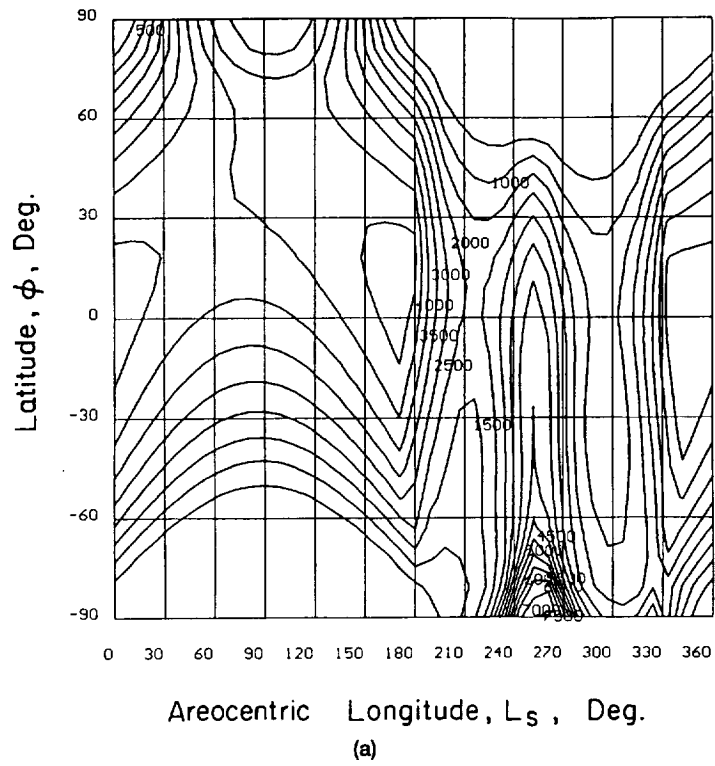
(a)

(b)
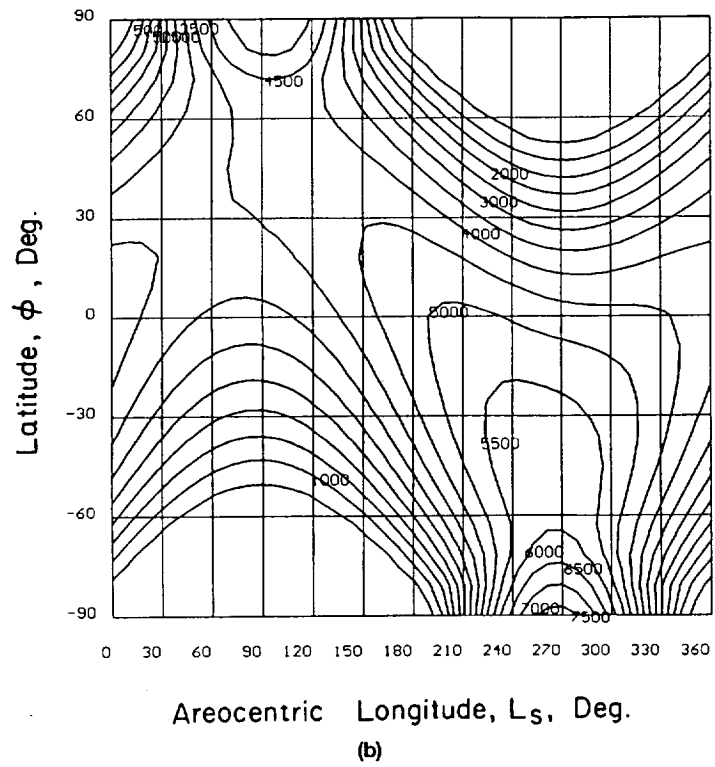
Fig. 13.—Variation of daily global insolation in (Whr/m^2) with latitude and areocentric longitude on EWPol tracking surface (inclination angle at local latitude); (a) based on optical depth junction (Eq. (1))^2, (b) based on $\tau = 0.5$.

21

REPORT DOCUMENTATION PAGE

Public reporting burden for this collection of information is estimated to average 1 hour per response, including the time for reviewing instructions, searching existing data sources, gathering and maintaining the data needed, and completing and reviewing the collection of information. Send comments regarding this burden estimate or any other aspect of this collection of information, including suggestions for reducing this burden, to Washington Headquarters Services, Directorate for Information Operations and Reports, 1215 Jefferson Davis Highway, Suite 1204, Arlington, VA 22202-4302, and to the Office of Management and Budget, Paperwork Reduction Project (0704-0188), Washington, DC 20503.

1. AGENCY USE ONLY (Leave blank)	2. REPORT DATE September 1994	3. REPORT TYPE AND DATES COVERED Technical Memorandum

4. TITLE AND SUBTITLE

Solar Radiation on Mars: Tracking Photovoltaic Array

5. FUNDING NUMBERS

WU–233–01–0A

6. AUTHOR(S)

Joseph Appelbaum, Dennis J. Flood, and Marcos Crutchik

7. PERFORMING ORGANIZATION NAME(S) AND ADDRESS(ES)

National Aeronautics and Space Administration
Lewis Research Center
Cleveland, Ohio 44135–3191

8. PERFORMING ORGANIZATION REPORT NUMBER

E–9062

9. SPONSORING/MONITORING AGENCY NAME(S) AND ADDRESS(ES)

National Aeronautics and Space Administration
Washington, D.C. 20546–0001

10. SPONSORING/MONITORING AGENCY REPORT NUMBER

NASA TM–106700

12a. DISTRIBUTION/AVAILABILITY STATEMENT

Unclassified - Unlimited
Subject Category 33

12b. DISTRIBUTION CODE

13. ABSTRACT (Maximum 200 words)

A photovoltaic power source for surface-based operation on Mars can offer many advantages. Detailed information on solar radiation characteristics on Mars and the insolation on various types of collector surfaces are necessary for effective design of future planned photovoltaic systems. In this article we have presented analytical expressions for solar radiation calculation and solar radiation data for single axis (of various types) and two axis tracking surfaces and compared the insolation to horizontal and inclined surfaces. For clear skies (low atmospheric dust load) tracking surfaces resulted in higher insolation than stationary surfaces, whereas for highly dusty atmospheres, the difference is small. The insolation on the different types of stationary and tracking surfaces depend on latitude, season and optical depth of the atmosphere, and the duration of system operation. These insolations have to be compared for each mission.

14. SUBJECT TERMS

Mars; Solar radiation; One and two axis tracking collectors

15. NUMBER OF PAGES
23

16. PRICE CODE
A03

17. SECURITY CLASSIFICATION OF REPORT Unclassified	18. SECURITY CLASSIFICATION OF THIS PAGE Unclassified	19. SECURITY CLASSIFICATION OF ABSTRACT Unclassified	20. LIMITATION OF ABSTRACT